AIMS Materials Science, 8(2): 221–246.
DOI: 10.3934/matersci.2021015
Received: 25 January 2021
Accepted: 17 March 2021
Published: 23 March 2021

http://www.aimspress.com/journal/Materials

Research article

Optimization of Bentocrete parameters using Response Surface Methodology (RSM)

M. Achyutha Kumar Reddy*, V. Ranga Rao, K. Naga Chaitanya, and Veerendrakumar C. Khed

Department of Civil Engineering, Koneru Lakshmaiah Education Foundation, Vaddeswaram, Guntur, India-522502

* **Correspondence:** Email: achyuthakumar@kluniversity.in.

Abstract: The present study aims at the influence of water/cement (W/C) ratio on workability, compressive strength, and durability, and microstructure of concrete by partial replacement of cement with bentonite (Bentocrete). The model development with the help of the matrix design was carried out using Response Surface Methodology (RSM). Scanning Electron Microscope (SEM) and X-ray diffraction used for assessment of bentonite microstructure. The variables in this research were water/cement (W/C) ratio and percentage of bentonite replacement. The W/C ratio was varied between 0.60 and 0.70; 0%, 10%, 20% and 30% of cement were substituted with bentonite. The responses (slump value, compaction factor, compressive strength (28 d), split tensile strength, flexural strength and charge passed through concrete (28 d) were assayed for all mixes. Design Expert 11.0 version was utilized for optimization using RSM. Bentonite's high-water absorption capacity decreased the workability as the OPC percentage decreased in the Bentocrete. The result has shown that the compressive strength, split tensile strength, and flexural strength of Bentocrete has decreased to 80% replacement of bentonite with OPC, increasing beyond that. This decrease is due to bentonite's pozzolanic reactivity. The durability of Bentocrete improved up to 20% replacement of OPC with bentonite. The increase is might be due to the pore filling effect, bentonite particles occupy the voids created by OPC since the particles of bentonite were finer than OPC. The models generated from RSM are valid with statistical significance in all the factors considered. 9.91% of the cost can be cut down at 80% cement substitution. The optimum solution with a desirability of 0.881

was obtained with 3.92% of bentonite substitution and 0.62 W/C ratio. The intended Bentocrete can be utilized in low-cost concrete production.

Keywords: water/cement ratio; bentonite; Bentocrete; optimization; Response Surface Methodology (RSM)

1. Introduction

In view of the importance of C–S–H gel formation in attaining strength in concrete, the addition of pozzolanic materials will help the cause as they are rich in SiO_2 [1]. The SiO_2 present in pozzolanic material will play a crucial role in secondary C–S–H gel reaction, which consumes the unreacted calcium in concrete [2]. Pozzolanic materials, in a broader sense, can be seen as two types for cement replacement, i.e., natural pozzolanic materials (e.g. bentonite) [3–6] and others are waste by-products from industries (e.g. Flyash, GGBS, and Silica Fume, etc.) [7]. While fly ash is a by-product of industries and has its physical and chemical characteristics more or less defined or consistent [8], natural pozzolanic materials will have their characteristics varied from region to region or even with in the same area sometimes [9]. One of the popular pozzolanic materials being utilized at a commercial level is fly ash [10].

The significant sources of fly ash are in general carbon-emitting sources which may not be sustainable in the long run [11]. So, the utilization of fly ash as a pozzolanic replacement of cement in concrete may not be sustainable, and we shall look at other pozzolanic materials that are from non-carbon emitting sources. Bentonite is a mineral admixture (Clay) and had plenty of applications in various fields. The major applications include the utilization of bentonite are as drilling fluids, foundry bonds, pelletizing iron ore, cat litter and absorbents [12]. In India, the significant applications of bentonite are in drilling and foundry fields. A tremendous amount of bentonite resources were located in Rajasthan (424 million tonnes) and Gujarath (134 million tonnes) states in India [13].

The researchers examined the strength of bentonite blended concrete (Bentocrete), variances in the results are were reported [14]. Bentonite is fine clay material; it shows different physical and chemical properties concerning the source of collection. Most of the research on Bentocrete was performed in Pakistan due to its abundance. Due to its variations in physicochemical properties, the performance of Bentocrete exhibits some uncertainties to the researchers. The average particle size of bentonite is nearly 4.32 μm [15]. It contains SiO_2 in high (45–65) percentages, and it shows pozzolanic properties. The specific gravity (2.6–2.85) of bentonite is lower than that of other pozzolanic materials [16]. The Bentocrete may perform less thermal resistance compared to other concretes made with pozzolanic materials like fly ash. It is attributed to the higher Loss of ignition (5–14) values of bentonite[10,14,16]. Bentocrete generally exhibited longer setting times when compared with cement paste [17–19].

The better performance of Bentocrete was observed when bentonite was preheated at 150 ^{o}C before mixing [3]. The strength activity index (SAI) of Bentocrete was found to be significantly less

during early curing days (7 d), increased gradually in later curing days (28 d) and was better than cement concrete there onwards [3,17,20]. Mirza et al., in 2009, observed that the SAI was better up to 21 percentage of bentonite blending after 28 d of curing because the pozzolans will actively participate in reaction in lateral ages [21]. The workability of bentonite blended concrete was decreased, inversely proportional to the percentage of blending [5]. Utilization of little amounts (1–2%) of sodium bentonite improves the workability of concrete upon proper mixing [12]. The water absorption of bentonite blended concrete was lesser than that of conventional concrete [3,4,22].

100% substitution of cement in Bentocrete will have feeble strength because of scarcity in binding agents like CaO (Citation). It is generally suggested that the replacement of cement in Bentocrete shall be in the range of 5–20% and should not be beyond 30% [23–26]. Bentocrete has a very little modulus of rupture values [3] and higher in the Fleuxural strength value [27,28]. Bentonite substitution (30–40%) increased the performance of concrete against Sulphate attack (Na_2SO_4 and $MgSO_4$) [3,29]. There was an increment in results was observed against acid attack (H_2SO_4 and HCl) [4,6]. Ventura et al. conducted tests to determine the effect of bentonite on corrosion protection of steel reinforcement, reported that bentonite addition increases the corrosion protection to steel [30]. Xie et al. held experiments by utilization of bentonite slurry, evaluated the mechanical properties of foamed concrete, almost the same strength were reported for the control mix, and 10% bentonite replaced mix [31].

Model advancement included the utilization of Response Surface Methodology (RSM) employing theories of mathematical and statistical analysis techniques between variables and responses [32]. Moreover, RSM was utilized for the optimization of the wanted set of objectives, either independent variables or responses [33,34]. RSM has additionally was used to implement multi-objective optimization in different concrete materials [35,36]. Bashar et al. performed multi-objective optimization to accomplish a connection between variables and responses of the properties of roller-compacted concrete by keeping fly ash content as constant, considering the combined effect of both crumb rubber and nano-silica [37]. Mohammed et al. utilized RSM to attain a relationship between variables (fly ash, nano-silica and superplasticizer) and responses (flow value, setting time and compressive strength) [38]. Baris et al. developed a graphical interface by utilizing RSM to determine the optimal weight of aggregates [20]. Geo et al. performed multi-response optimization by keeping alkali activator concentration and liquid-solid ratio as variables, 2 h and 3 h curing as responses [39]. Long et al. performed multi-objective optimization by restraining action of corrosion, fatigue and fiber content as independent variables and compressive strength, flexural strength and dynamic elastic modulus as responses [40].

In general, the bentonite will attain its normal consistency at more water consumption than that of cement and fly ash due to its high-water absorption capacity. This will have an impact on water-cement ratios to be used during concrete mix design [21]. So, the current research on the effect of water cement-ratio on workability, compressive strength, split tensile strength, flexural strength and durability of concrete with different proportions of cement replacements with bentonite. The role of bentonite and water-cement ratio was assessed based on the RSM. Also, the study attempts to compare the costs involved in using bentonite as a replacement for cement.

2. Materials and methods

2.1. Materials

In this research OPC-43 grade cement was used as per ASTM C150M, bentonite was collected from Unique bleaching clay (17°14′27″N and 77°35′14″E), Tandur (southern region of India). Table 1 shows the chemical analysis and physical properties of bentonite and cement. The quality of the water used for this study was within limits as per ASTM C1602M. In this study, the fine aggregate and coarse aggregate was used as per the standard procedure ASTM C33/C33M-18.

Table 1. Chemical analysis and physical properties of bentonite and cement.

S. No.	Component	Chemical composition%	
		Bentonite	Cement
1	SiO_2	51.11	18.6
2	Al_2O_3	16.38	8.17
3	CaO	7.12	62.5
4	MgO	7.57	1.43
6	Fe_2O_3	7.65	3.26
7	K_2O	1.34	1.09
8	Na_2O	0.29	0.71
9	P_2O_5	0.29	0.07
10	MnO	0.14	-
11	V_2O_5	0.07	-
12	TiO_2	1.29	-
13	SO_3	-	2.63
	Physical properties		
14	Blain fineness (cm^2/gm)	1730	4750
15	Specific gravity	3.12	2.79
16	Initial setting time (min)	-	90
17	Final setting time (min)	-	345
18	Loss on Ignition	6.75	1.23

2.1.1. SEM and XRD analysis of bentonite

The XRD analysis was performed by using X-Pert X-ray Diffractometer of PANalytical, model number: PW 3040/00. The investigation was conducted at a 2-theta range of 10–80 with a step size of 0.5 and a 5 degrees/min scan rate. The results (Figure 1) have shown different phases that can be further identified as five mineral crystalline structures. The calcite mineral has established a prominent presence in the XRD. Scanning electron microscopy (SEM) images were obtained by using Nova Nano SEM/FEI for further pursuit. The SEM images (Figure 2) have also shown the presence of crystalline structures in the bentonite sample.

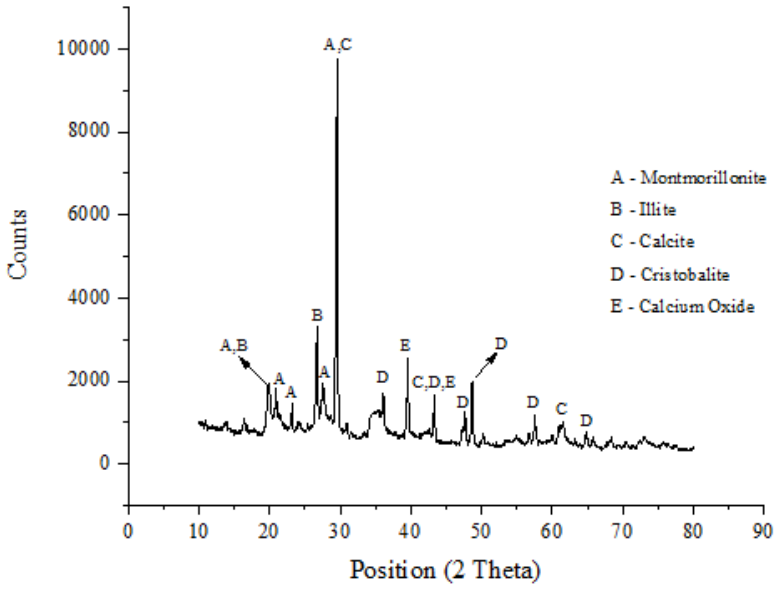

Figure 1. XRD Analysis of bentonite.

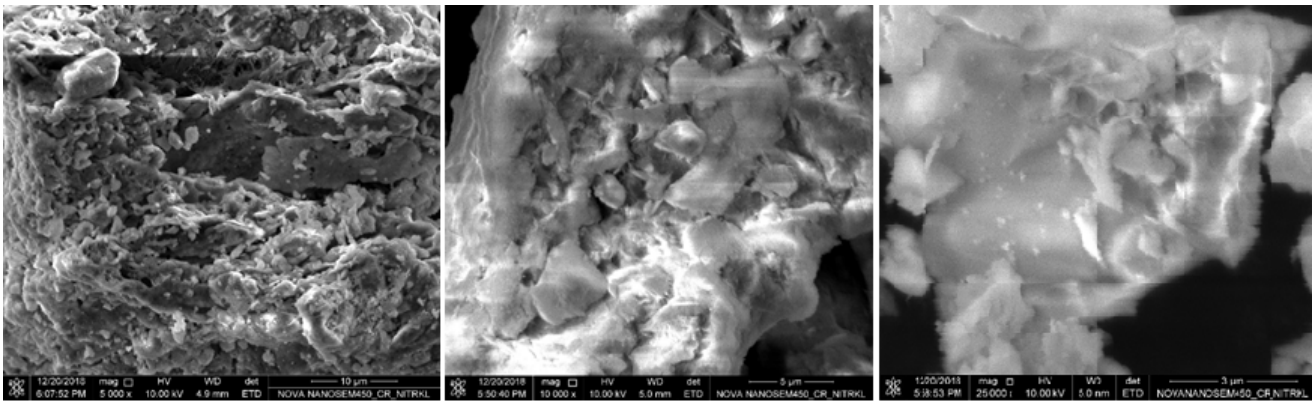

Figure 2. SEM Analysis of bentonite.

2.2. Testing of specimens

The standard consistency test was conducted on cement paste to determine the optimum water content for getting maximum strength with the Vicat apparatus as per standard procedure ASTM C187. Compressive strength of cement mortar tested for all mixes as per ASTM C109. The workability of all Bentocrete mixes were determined by slump cone test, and compaction factor test as per standard procedures ASTM C143 and IS 1199:1959. For determination of compressive strength, a total number of 396 concrete cubes (150 mm × 150 mm × 150 mm) were cast and tested to failure at different ages of concrete (7, 28 and 56 d) as per the standard procedure ASTM C39. Split tensile strength test was performed to determine the split tensile strength of Bentocrete mixes as per the standard procedure ASTM C496, a total number of 132 cylinders (150 mm × 300 mm) were cast and tested to failure after 28 d curing. Flexural strength test was performed to determine the

flexural strength as per the standard procedure ASTM C78, a total number of 132 specimens (150 mm × 150mm × 700 mm) were cast and tested to failure (third-point loading) after 28 d curing. Rapid chloride ion penetration test was performed to determine chloride ion penetration into Bentocrete as per standard procedure ASTM C 1202-97. A total number of 528 specimens, 44 sets (a set include four samples) were tested against chloride ion permeability after 7, 28 and 56 curing; respectively, Figure 3 represents the rapid chloride penetration test setup. The mix design of each mix was prepared as per ACI committee 211; the details of each blend were shown in Table 2.

Figure 3. Setup for rapid chloride penetration test.

Table 2. The mix design details of all mixes.

Si No.	Mix name	Cement (kg)	Bentonite (kg)	Fine aggregate (kg)	Coarse aggregate (kg)	Water (L)	Ratio
1	CM60	320	0	819.299	1077.072	192	1:2.56:3.37
2	CM61	320	0	819.265	1068.34	195.2	1:2.56:3.34
3	CM62	320	0	819.197	1059.643	198.4	1:2.56:3.31
4	CM63	320	0	819.096	1050.981	201.6	1:2.56:3.28
5	CM64	320	0	818.961	1042.355	204.8	1:2.56:3.26
6	CM65	320	0	818.793	1033.763	208	1:2.56:3.23
7	CM66	320	0	818.592	1025.207	211.2	1:2.56:3.20
8	CM67	320	0	818.357	1016.685	214.4	1:2.56:3.18
9	CM68	320	0	818.088	1008.088	217.6	1:2.56:3.15
10	CM69	320	0	817.787	999.748	220.8	1:2.56:3.12
11	CM70	320	0	817.452	991.332	224	1:2.55:3.10

Continued on next page

Si No.	Mix name	Cement (kg)	Bentonite (kg)	Fine aggregate (kg)	Coarse aggregate (kg)	Water (L)	Ratio
12	10BC60	288	32	818.145	1075.548	192	1:2.56:3.36
13	10BC61	288	32	815.54	1063.482	195.2	1:2.55:3.32
14	10BC62	288	32	815.68	1055.8	198.4	1:2.55:3.30
15	10BC63	288	32	816.27	1047.365	201.6	1:2.55:3.27
16	10BC64	288	32	815.18	1037.55	204.8	1:2.55:3.24
17	10BC65	288	32	815.23	1029.27	208	1:2.55:3.22
18	10BC66	288	32	814.98	1019.54	211.2	1:2.55:3.19
19	10BC67	288	32	814.77	1012.23	214.4	1:2.55:3.16
20	10BC68	288	32	814.48	1003.74	217.6	1:2.55:3.14
21	10BC69	288	32	814.169	995.325	220.8	1:2.54:3.11
22	10BC70	288	32	816.29	994.29	224	1:2.55:3.11
23	20BC60	256	64	812.346	1067.931	192	1:2.54:3.34
24	20BC61	256	64	812.215	1058.625	195.2	1:2.54:3.31
25	20BC62	256	64	812.18	1050.568	198.4	1:2.54:3.28
26	20BC63	256	64	812.04	1041.939	201.6	1:2.54:3.26
27	20BC64	256	64	811.827	1034.547	204.8	1:2.54:3.23
28	20BC65	256	64	811.783	1024.787	208	1:2.54:3.20
29	20BC66	256	64	811.689	1016.561	211.2	1:2.54:3.18
30	20BC67	256	64	811.263	1008.368	214.4	1:2.54:3.15
31	20BC68	256	64	810.885	988.38	217.6	1:2.53:3.09
32	20BC69	256	64	810.552	990.903	220.8	1:2.53:3.10
33	20BC70	256	64	810.185	982.52	224	1:2.53:3.07
34	30BC60	224	96	812.513	1059.536	192	1:2.54:3.31
35	30BC61	224	96	812.415	1050.87	195.2	1:2.54:3.28
36	30BC62	224	96	812.285	1042.241	198.4	1:2.54:3.26
37	30BC63	224	96	811.921	1039.418	201.6	1:2.54:3.25
38	30BC64	224	96	811.544	1029.841	204.8	1:2.54:3.22
39	30BC65	224	96	811.229	1020.299	208	1:2.54:3.19
40	30BC66	224	96	811.088	1011.792	211.2	1:2.53:3.16
41	30BC67	224	96	810.87	1003.914	214.4	1:2.53:3.14
42	30BC68	224	96	810.53	995.77	217.6	1:2.53:3.11
43	30BC69	224	96	810.282	987.66	220.8	1:2.53:3.09
44	30BC70	224	96	810.007	985.457	224	1:2.53:3.08

2.3. Specimen designation

Two types of nomenclatures were framed for simple identification of the mixes. Each specimen was represented by the percentage of partial replacement followed by bentonite cement (BC) followed by water/cement ratio multiplied with 100. For example, 20BC68 represents 20% of cement was replaced by bentonite with 0.68 as water/cement ratio, 10BC represents 10% of cement was replaced by calcium bentonite, control mix (CM) represents 0BC hence no blending of bentonite in that mix.

3. Results and discussion

3.1. Normal consistency of cement paste

The determination of normal consistency for any cement is essential, the water content of paste which will produce the desired consistency. The consistency of cement was directly proportional to the percentage of bentonite blended, as shown in Figure 4. There is a strong linear correlation between percentage replacement of bentonite and normal consistency with R^2 values reaching up to 0.99. According to the analysis, there is an approximately 2.5% increase in normal consistency for every 1% increase in cement replacement with bentonite; this attributes the bentonite's high water absorption capacity [12].

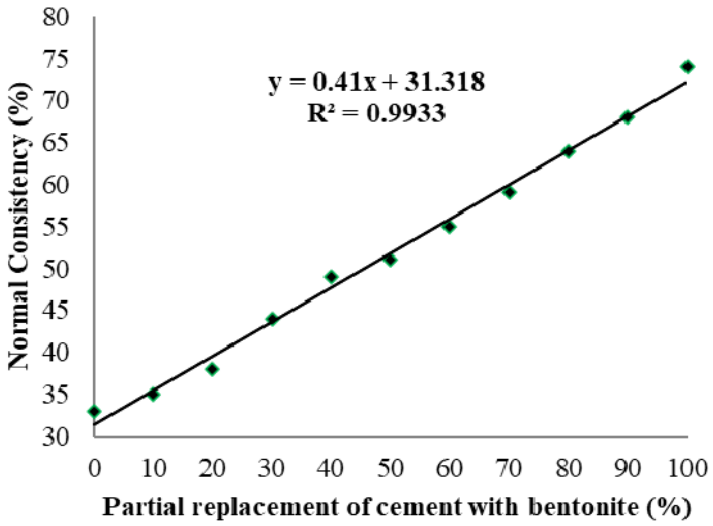

Figure 4. Normal consistency of bentonite mixtures.

3.2. Compressive strength of cement mortar

The compressive strength of hardened cement is the property of the material that is required for structural use. Figure 5 shows the compressive strengths of hardened cement mixes; maximum compressive strength was demonstrated by 10% bentonite blended mix. The strength of hardened cement mixes was examined as per standard procedure IS:650. In cement mortar mixes, 10BC and 30BC exhibits 6.41% higher and 17.00% less compressive strengths than CM.

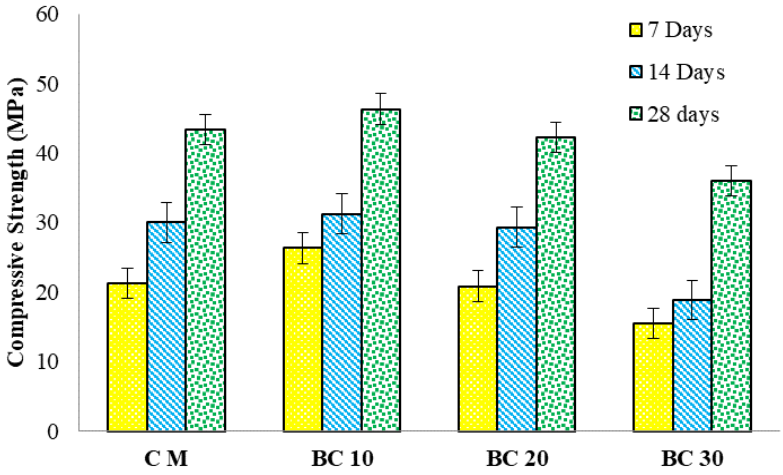

Figure 5. Compressive strength (MPa) of mixes at different ages.

3.3. Workability of concrete

The workability was delineated as determination of the ease of placement and resistance to the segregation of concrete. The workability was determined by the help of a slump cone test, and compaction factor test, slump values and compaction factor were measured for each mix. 45 mm slump value was fixed by the help of trail mixes for CM61, remaining values measured while casting of each mix. The results were drawn after testing of all specimens (section testing of specimens), Figure 6 shows the slump values of all mixes.

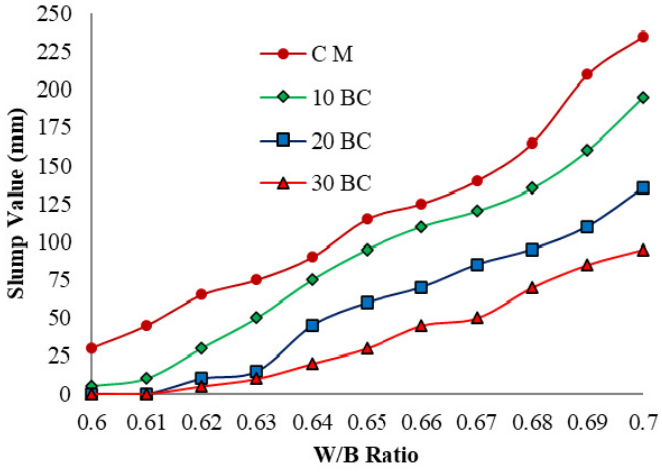

Figure 6. Slump values of all bentonite mixes.

The degree of compaction is known as compaction factor, the ratio of achieved density of the concrete in the same at compacted state. The results were taken after performing the test for all mixes; Figure 7 shows the compaction factor values. The workability of blended mixes was reduced as the percentage of bentonite blending increased. This can be attributed to the high-water absorption capacity of bentonite. The lowest workability was observed with a 30BC60 mix. The causative is the

combination of higher replacement (30%) of cement with bentonite and low water-cement ratio (0.60). Simultaneously, the highest workability was observed with CM70. The workability of blended mixes was reduced as the percentage of bentonite blending increased.

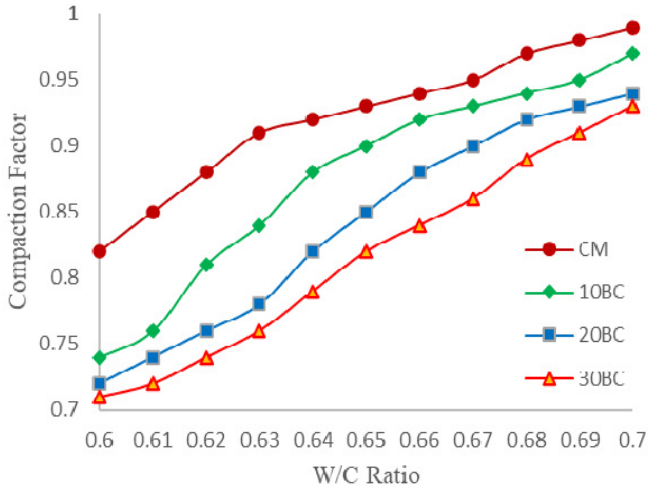

Figure 7. Compaction factor values of all bentonite mixes.

3.4. Compressive strength of concrete

The compressive strength of concrete is always a crucial aspect of structural design and is specified for compliance purposes. The compressive strength of all mixes is inversely proportional to the water-cement ratio as per the basic principle of concrete [21].

Figure 8 shows the compressive strength of a set of all specimens (Table 2) after seven days of curing. CM mixes shown higher compressive strength among was all, because of 43-grade cement's property to gain early age strength [21]. The pozzolanic materials like bentonite will tend not to have early age compressive strength. Thus, the mixes with high bentonite show less compressive strength.

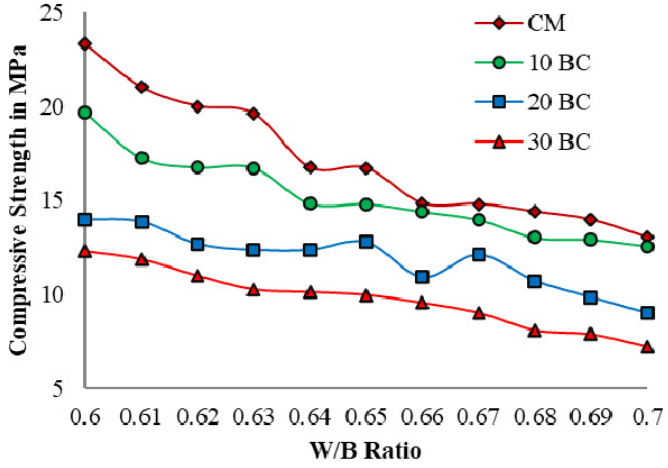

Figure 8. Compressive strength of bentonite mixes at the age of 7 d.

Figure 9 shows the compressive strength of a set of all specimens (Table 2) after 28 d of curing. There is an improvement in the compressive strength of bentonite mixes as the curing days were increased. The compressive strength of 10BC mixtures increases and nearly equals with CM. The occurrence of pozzolanic reactions may result in the improvement of the compressive strength for all bentonite mixes. The increase in the percentage of strength for 20BC and 30BC was observed, but those mixes showed lower compressive strength than that of CM.

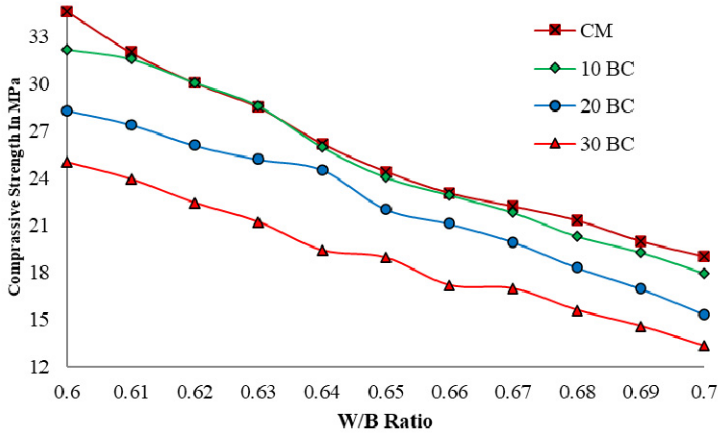

Figure 9. Compressive strength of bentonite mixes at the age of 28 d.

Figure 10 shows the compressive strength of a set of all specimens (Table 2) after 56 d of curing. The compressive strength of 10BC and 20BC shown higher than CM. 10BC and 30BC shown highest and lowest compressive strength among all mixes, whereas 20BC shown greater than CM. A little amount of strength gain percentage was observed for CM. It can be assessed that bentonite fills the voids among cement particles in concrete (pore filling effect) and a pozzolanic reaction is taking place between inactive calcium in OPC and excess of SiO_2 present in bentonite.

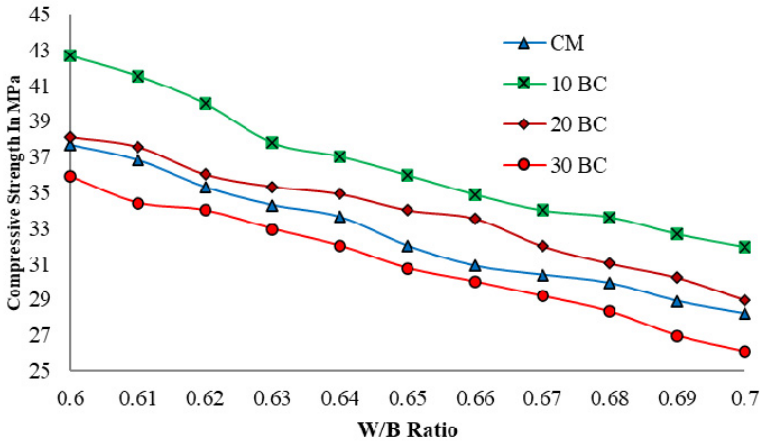

Figure 10. Compressive strength of bentonite mixes at the age of 56 d.

The compressive strength needs to increase as workability decreases, as per the fundamentals of concrete. In this study, this fundamental was applied up to 20% replacement of bentonite. It can be attributed to pore filling effect and pozzolanic reaction with bentonite. The introduction of bentonite in 30 percentage does not follow the fundamentals. Those mixes show a decrease in strength as well as workability. The causative is less CaO content presence in bentonite than cement (Table 1) and the assimilating bentonite behaviour.

3.5. Split tensile strength of concrete

In the split tensile strength test, a cylinder was placed in compression testing, and it was tested up to failure. Figure 11 shows the split tensile strength of all bentonite mixes. CM has demonstrated better performance than other mixes; equal split tensile strength was observed in a few 10BC mixes compared with CM. 30BC shown lower performance among all mixes. It was observed that split tensile strength was decreasing in the case of more than 20% of bentonite blending. It can be assessed that the poor bond formation between bentonite and cement particles.

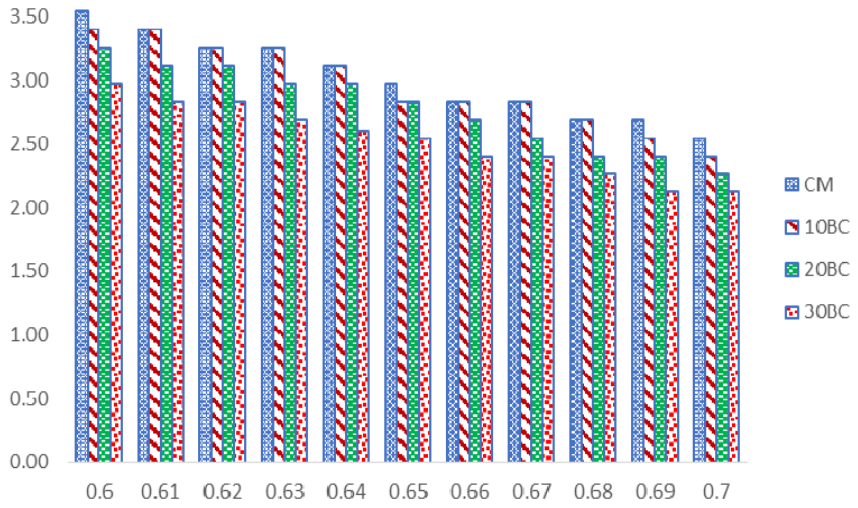

Figure 11. Split tensile strength of bentonite mixes.

3.6. Flexural strength of concrete

In the flexural strength test, a plain concrete beam is subjected to flexure using third-point loading test. Figure 12 shows the flexural strength of all bentonite mixes. CM exhibits better flexural strength than other mixes comparatively. Few 10BC mixes shown equal flexural strength. The flexural strength of concrete is inversely proportional to bentonite blending (after 20%) and W/C ratio. It can be attributed to the week bond formation between bentonite and cement particles.

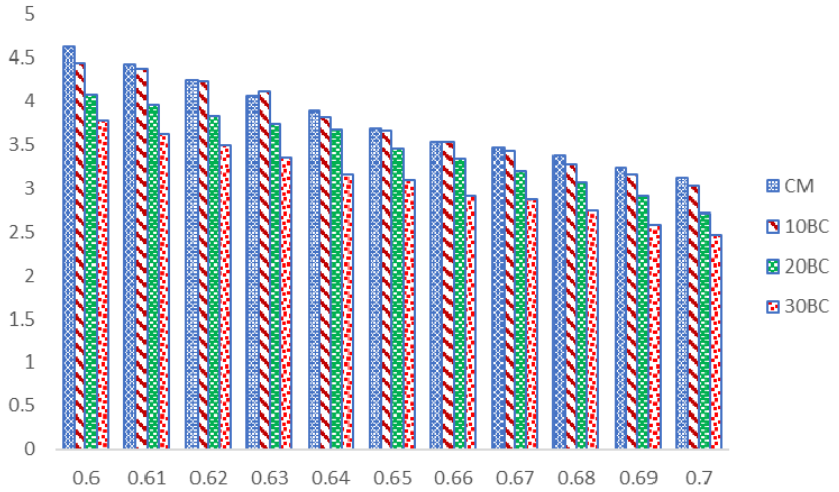

Figure 12. Flexural strength of bentonite mixes.

3.7. Rapid chloride penetration test (RCPT) of concrete

Figure 13 shows the average charge (Columbus) passed through 4 cells after seven days of curing. CM exhibits less Charge Passed (CP) (1200–1250) through it compared to others. All bentonite substituted mixes shown poor performance against chloride ion penetration at the age of seven days. This result may be because the pozzolanic reaction will not happen within seven days. The chloride ion penetration was decreased by increasing the water-cement ratio.

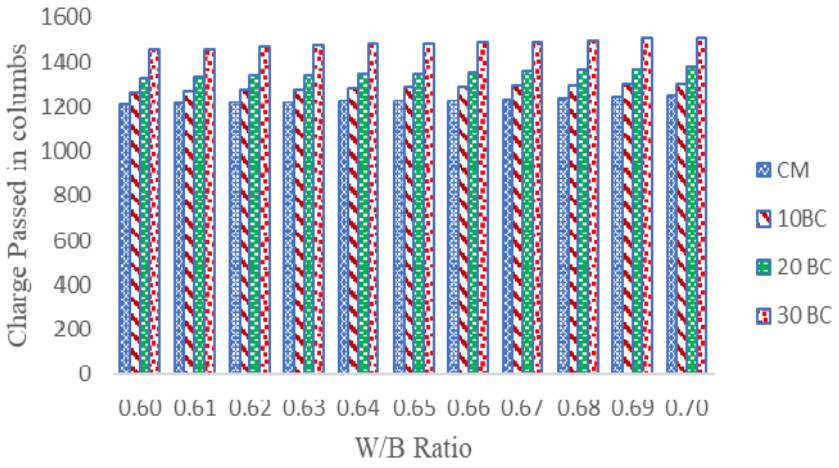

Figure 13. Charge passed in concrete after 7 d curing.

Figure 14 shows the average charge passed through 4 cells after 28 d curing. 10 BC exhibits less CP (360–410) through it comparatively with other mixes. 30 BC has shown abysmal performance against chloride ion penetration. This may attribute the occurrence of pozzolanic reaction at lateral (28 d) ages.

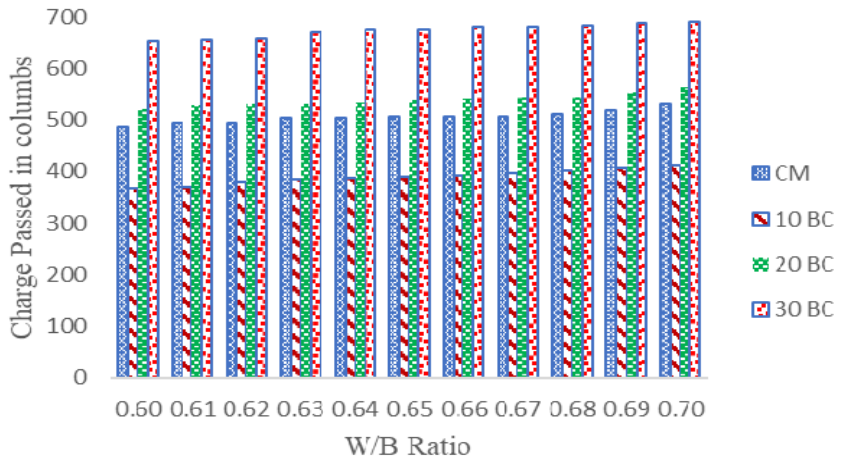

Figure 14. Charge passed in concrete after 28 d curing.

Figure 15 shows the average charge passed through 4 cells after 56 d curing. 10 BC exhibits less CP (290–320) through it comparatively with other mixes. CM and 20BC performed 30 BC shown abysmal performance against chloride ion penetration. This may attribute the occurrence of pozzolanic reaction at lateral (56 d) ages.

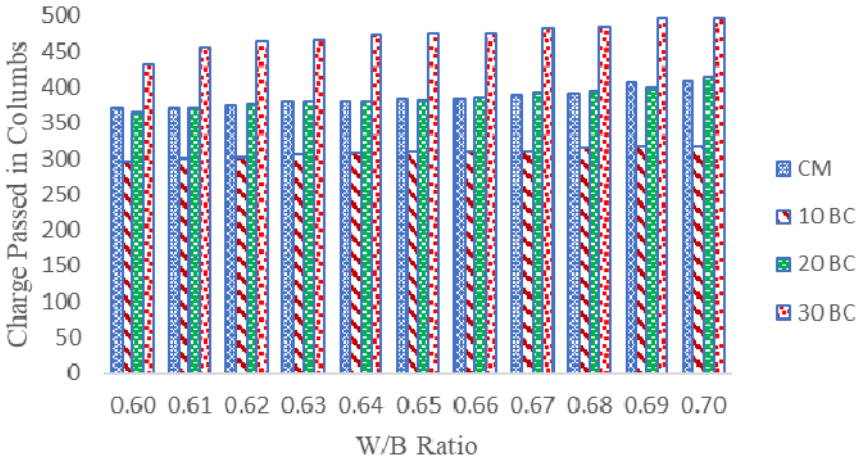

Figure 15. Charge passed in concrete after 56 d curing.

3.8. Cost analysis

Lesser cost is one of the reasons to blend bentonite with cement. The bentonite was brought from the company named "Unique Bleaching Clay" located at Tandur in Telangana state in India. The cost comparison was made according to "Standard Schedules of Rates" (SSR), Andhra Pradesh-2018-19, India, the points of interest of the cost of all blends have appeared in Table 3.

Table 3. Cost comparison of all mixes per cubic meter.

Description of item	CM		10BC		20BC		30BC	
	Quantity	Price	Quantity	Price	Quantity	Price	Quantity	Price
OPC (kg)	320	2240	288	2016	256	1026	224	896
Calcium bentonite (kg)	0	0	32	32	64	64	96	96
Fine aggregate (m^3)	819.2	148.7	818.1	148.7	812.3	148.7	812.5	148.7
Coarse aggregate (m^3)	1077.0	487.6	1075.5	487.6	1067.9	487.6	1059.5	487.6
Total price in Indian rupees		2876.3		2684.3		2492.4		2312.9

4. RSM modeling

4.1. Development of the model

In RSM, various types of models are available like Central Composite, Box Behnken and optimal (custom) in a randomized design. Choosing a model type depends on the nature of accessible information and levels for each factor. For the most part, for an experiment matrix that has been as of now built up, the historical data or user-defined model or is applied for the development and investigation of a model [41]. The linear model is signified by the first order as shown in Eq 1. Similarly, polynomial models were signified by the second order as shown in Eq 2.

$$y = \beta_0 + \beta_1 X_1 + \beta_2 X_2 + \beta_3 X_3 + \cdots\cdots + \beta_n X_n + \varepsilon \quad (1)$$

where y represents the response modeled, β_0 is the y-intercept at $X_1 = X_2 = 0$, whereas β_1 and β_2 are the coefficients of first and second independent variables, respectively, while X_1 and X_2 are the first and second independent variables, and Ɛ is the error.

$$y = \beta_0 + \sum_{i=1}^{k} \beta_i X_i + \sum_{i=1}^{k} \beta_{ii} X_j^2 + \sum_{j=2}^{k} \sum_{i=1}^{j=1} \beta_{ij} X_i X_j + \varepsilon \quad (2)$$

where y represents the response's model, the coded values of independent variables are represented by X_i and X_j, i and j are the coefficients for the linear and quadratic equations, respectively, β_o stands for the y-intercept at $X_1 = X_2 = 0$, whereas k represents the number of independent variables used in the analyses, and Ɛ is the error [41].

4.2. Mix matrix design

Design Expert 11.0 version was used for modelling in this investigation. The design of experiments was generated using central composite design method based on two variables (bentonite replacement and W/C ratio). Four levels of % of bentonite replacement (0%, 10%, 20% and 30%) and ten levels of W/C ratio (0.60, 0.61, 0.62, 0.63, 0.64, 0.65, 0.66, 0.67, 0.68, 0.69 and 0.70) were used. A total number of 44 combinations of mixtures was developed in RSM. Table 4 represents the details of all mixtures and their combination of variables. The responses of bentonite blended

concrete (slump value, compaction factor, CS 28 d, split tensile strength, flexural strength and 28 d CP) were determined for all mixtures, considered for RSM analysis and optimization.

Table 4. Design matrix of experiments and responses.

Run	F:1	F:2	R1	R2	R3	R4	R5	R6
	Bentonite substitution (%)	W/C	Slump value (mm)	Compactor factor	CS 28 d (MPa)	Split tensile strength (MPa)	Flexural strength (MPa)	CP 28 d (Columbus)
1	0	0.6	30	0.82	34.65	3.54	4.63	488.3
2	0	0.61	45	0.85	32.04	3.40	4.43	494.3
3	0	0.62	65	0.88	30.09	3.26	4.25	495.0
4	0	0.63	75	0.91	28.54	3.26	4.06	503.8
5	0	0.64	90	0.92	26.22	3.11	3.89	505.5
6	0	0.65	115	0.93	24.44	2.97	3.69	506.5
7	0	0.66	125	0.94	23.07	2.83	3.54	507.0
8	0	0.67	140	0.95	22.22	2.83	3.47	508.0
9	0	0.68	165	0.97	21.33	2.69	3.38	511.5
10	0	0.69	210	0.98	20.00	2.69	3.24	519.5
11	0	0.7	235	0.99	19.03	2.55	3.13	532.0
12	10	0.6	5	0.74	32.23	3.40	4.45	367.5
13	10	0.61	10	0.76	31.62	3.40	4.38	369.5
14	10	0.62	30	0.81	30.12	3.26	4.23	379.0
15	10	0.63	50	0.84	28.63	3.26	4.12	384.0
16	10	0.64	75	0.88	26.02	3.11	3.83	388.3
17	10	0.65	95	0.9	24.09	2.83	3.66	390.8
18	10	0.66	110	0.92	22.96	2.83	3.54	391.0
19	10	0.67	120	0.93	21.85	2.83	3.43	396.0
20	10	0.68	135	0.94	20.34	2.69	3.28	403.3
21	10	0.69	160	0.95	19.32	2.55	3.17	407.0
22	10	0.7	195	0.97	17.99	2.41	3.03	411.8
23	20	0.6	0	0.72	28.33	3.26	4.08	521.5
24	20	0.61	0	0.74	27.44	3.11	3.96	529.5
25	20	0.62	10	0.76	26.11	3.11	3.84	532.5
26	20	0.63	15	0.78	25.22	2.97	3.74	533.0
27	20	0.64	45	0.82	24.56	2.97	3.68	535.5
28	20	0.65	60	0.85	22.05	2.83	3.46	540.8
29	20	0.66	70	0.88	21.12	2.69	3.33	541.8
30	20	0.67	85	0.9	19.96	2.55	3.21	543.8
31	20	0.68	95	0.92	18.34	2.41	3.07	545.8
32	20	0.69	110	0.93	17	2.41	2.91	555.8
33	20	0.7	135	0.94	15.37	2.26	2.72	563.5
34	30	0.6	0	0.71	25.03	2.97	3.78	655.8
35	30	0.61	0	0.72	23.96	2.83	3.63	657.0
36	30	0.62	5	0.74	22.45	2.83	3.5	659.3
37	30	0.63	10	0.76	21.23	2.69	3.35	673.3
38	30	0.64	20	0.79	19.43	2.60	3.17	676.3
39	30	0.65	30	0.82	18.96	2.55	3.1	677.5
40	30	0.66	45	0.84	17.2	2.41	2.91	683.0
41	30	0.67	50	0.86	16.99	2.41	2.87	683.5
42	30	0.68	70	0.89	15.62	2.26	2.74	684.3
43	30	0.69	85	0.91	14.6	2.12	2.58	689.5
44	30	0.7	95	0.93	13.33	2.12	2.47	691.8

4.3. Analysis of variance

The summaries of ANOVA for the responses of the Bentocrete properties (slump value, compaction factor, CS 28 d, split tensile strength, flexural strength and 28 d CP) were shown in Tables 5–11. The models' F-values are 553.10, 363.29, 550.10, 381.30, 609.69 and 5635.79 for slump value, compaction factor, CS 28 d, split tensile strength, flexural strength and 28 d CP respectively, pointing all models to be significant, with 0.01% chances for all models. The Confidence Interval (CI) of the data presented in the model is 95%. This could be used to find out the significance of all the models and their terms. For slump value and split tensile strength, a quadratic model was used, and A, B, AB, A^2, B^2 were the terms, as per the p-value of 0.05. The significant models of compaction factor, CS 28 d, flexural strength, and CP 28 d, and its terms were cubic and, A, B, AB, A^2, B^2, A^2B, AB^2, A^3 and, B^3, respectively, based on the p-values were less than 0.05.

Table 5. ANOVA for Quadratic model, R1: slump value.

Source	Sum of squares	df	Mean square	F-value	p-value	
Model	1.550E + 05	5	31007.90	553.10	<0.0001	significant
A-bentonite replacement	41319.20	1	41319.20	737.02	<0.0001	
B-water/cement ratio	1.063E + 05	1	1.063E + 05	1896.65	<0.0001	
AB	5923.68	1	5923.68	105.66	<0.0001	
A^2	205.11	1	205.11	3.66	0.0633	
B^2	1260.61	1	1260.61	22.49	<0.0001	
Residual	2130.37	38	56.06			
Cor total	1.572E + 05	43				

Table 6. ANOVA for Cubic model, R2: compaction factor.

Source	Sum of squares	df	Mean square	F-value	p-value	
Model	0.2826	9	0.0314	363.29	<0.0001	significant
A-bentonite replacement	0.0068	1	0.0068	78.30	<0.0001	
B-water/cement ratio	0.0332	1	0.0332	384.19	<0.0001	
AB	0.0030	1	0.0030	35.00	<0.0001	
A^2	0.0012	1	0.0012	13.91	0.0007	
B^2	0.0027	1	0.0027	31.56	<0.0001	
A^2B	0.0017	1	0.0017	19.44	<0.0001	
AB^2	0.0011	1	0.0011	12.23	0.0013	
A^3	4.091E-06	1	4.091E-06	0.0473	0.8291	
B^3	0.0001	1	0.0001	0.8009	0.3771	
Residual	0.0029	34	0.0001			
Cor total	0.2856	43				

Table 7. ANOVA for Cubic model, R3: CS 28 d

Source	Sum of squares	df	Mean square	F-value	p-value	
Model	1150.93	9	127.88	550.10	< 0.0001	significant
A-bentonite replacement	24.93	1	24.93	107.24	< 0.0001	
B-water/cement ratio	113.81	1	113.81	489.57	< 0.0001	
AB	9.70	1	9.70	41.74	< 0.0001	
A^2	20.78	1	20.78	89.40	< 0.0001	
B^2	2.49	1	2.49	10.71	0.0025	
A^2B	0.4925	1	0.4925	2.12	0.1547	
AB^2	2.54	1	2.54	10.94	0.0022	
A^3	1.19	1	1.19	5.12	0.0302	
B^3	0.1151	1	0.1151	0.4951	0.4865	
Residual	7.90	34	0.2325			
Cor total	1158.84	43				

Table 8. ANOVA for Quadratic model, R4: split tensile strength.

Source	Sum of squares	df	Mean square	F-value	p-value	
Model	5.66	5	1.13	381.30	<0.0001	significant
A-bentonite replacement	1.46	1	1.46	492.99	<0.0001	
B-water/cement ratio	4.08	1	4.08	1374.26	<0.0001	
AB	0.0052	1	0.0052	1.74	0.1954	
A^2	0.1108	1	0.1108	37.31	<0.0001	
B^2	0.0007	1	0.0007	0.2208	0.6411	
Residual	0.1129	38	0.0030			
Cor total	5.78	43				

Table 9. ANOVA for Cubic model, R5: flexural strength.

Source	Sum of squares	df	Mean square	F-value	p-value	
Model	12.07	9	1.34	609.69	<0.0001	significant
A-bentonite replacement	0.2878	1	0.2878	130.83	<0.0001	
B-water/cement ratio	1.12	1	1.12	510.87	<0.0001	
AB	0.0305	1	0.0305	13.86	0.0007	
A^2	0.2490	1	0.2490	113.18	<0.0001	
B^2	0.0114	1	0.0114	5.17	0.0294	
A^2B	0.0006	1	0.0006	0.2902	0.5936	
AB^2	0.0172	1	0.0172	7.81	0.0085	
A^3	0.0139	1	0.0139	6.33	0.0168	
B^3	0.0006	1	0.0006	0.2662	0.6093	
Residual	0.0748	34	0.0022			
Cor total	12.15	43				

Table 10. ANOVA for Cubic model, R6: CP 28 d.

Source	Sum of squares	df	Mean square	F-value	p-value	
Model	4.626E + 05	9	51397.11	5635.79	<0.0001	significant
A-bentonite replacement	1.050E + 05	1	1.050E+05	11509.10	<0.0001	
B-water/cement ratio	388.24	1	388.24	42.57	<0.0001	
AB	0.0525	1	0.0525	0.0058	0.9399	
A^2	1.745E+05	1	1.745E + 05	19135.34	<0.0001	
B^2	0.4838	1	0.4838	0.0531	0.8192	
A^2B	8.67	1	8.67	0.9502	0.3365	
AB^2	38.92	1	38.92	4.27	0.0465	
A^3	43851.07	1	43851.07	4808.35	<0.0001	
B^3	116.64	1	116.64	12.79	0.0011	
Residual	310.07	34	9.12			
Cor total	4.629E + 05	43				

Table 11. Validation of models.

Response	R^2	Adj. R^2	Pred. R^2	Adj.R^2-Pred.R^2	SD	Adeq.	Mean
Slump value	0.9864	0.9847	0.9821	0.0026	7.49	85.9629	75.34
Compaction factor	0.9897	0.9870	0.9802	0.0068	0.0093	62.4137	0.8634
28 d CS	0.9932	0.9914	0.9873	0.0041	0.4821	91.3261	22.98
Split tensile strength	0.9805	0.9779	0.9743	0.0036	0.0545	72.18	2.82
Flexural strength	0.9938	0.9922	0.9889	0.0033	0.0469	96.7725	3.52
CP 28 d	0.9993	0.9992	0.9988	0.0004	3.02	225.9156	528.03

For slump value, A^2 was the insignificant term and interaction in the quadratic model. The insignificant terms in compaction factor model were A^3 and B^3, while A^2B and B^3 were insignificant terms in CS 28 d cubic model, whereas the insignificant terms in split tensile strength quadratic model were AB and B^2. The insignificant terms in flexural strength cubic model were A^2B and B^3, whereas AB, B^2 and A^2B were insignificant terms in CP 28 d. A few interactions were not significant in all bentonite mixes influencing factors because of their higher (>0.05) p-values. The positive and negative signs were assigned in the models and their interactions to show the effects of the variables on all bentonite mixes factors.

The final models for slump value, compaction factor, CS 28 d, split tensile strength, flexural strength and 28 d CP of all mixes comprising all the terms are presented in Eqs 3–8, respectively.

$$\text{Slump value} = +1342.72727 + 17.94318\,A - 5831.96970\,B - 32.81818\,AB + 0.021591\,A^2 + 6060.60606\,B^2 \quad (3)$$

$$\text{Compaction factor} = +7.45830 + 0.151008\,A - 44.12313\,B - 0.563364\,AB + 0.001302\,A^2 + 86.85606\,B^2 - 0.001955\,A^2B + 0.496503\,AB^2 + 4.54545E-07\,A^3 - 52.93318\,B^3 \quad (4)$$

$$\text{CS 28 d} = -196.85548 - 10.37951\,A + 1752.40855\,B + 31.98212\,A\,B - 0.039650\,A^2 - 3573.76457\,B^2 + 0.033455\,A^2B + 0.000245\,A^3 + 2158.11966\,B^3 \quad (5)$$

$$\text{Spilt tensile strength} = +7.73014 - 0.021167\,A - 4.40756\,B + 0.030625\,AB - 0.000502\,A^2 - 4.37166\,B^2 \quad (6)$$

$$\text{Flexural strength} = -8.19684 - 0.856959\,A + 117.10348\,B + 2.63983\,AB - 0.002728\,A^2 - 251.96096\,B^2 + 0.001205\,A^2B - 2.00117\,AB^2 + 0.000027\,A^3 + 153.94328\,B^3 \quad (7)$$

$$\text{CP 28 d} = -17862.46208 - 77.38314\,A + 85306.42113\,B + 128.13371\,AB + 2.83872\,A^2 - 1.32425E+05\,B^2 - 0.140341\,A^2B - 95.25058\,AB^2 - 0.047061\,A^3 + 68703.86558\,B^3 \quad (8)$$

The properties of formulated models of for slump value, compaction factor, CS 28 d, split tensile strength, flexural strength and 28 d CP of all mixes were presented in Table 11. The adequacy of the formulated models was validated by their degree of correlation (R^2). A high degree of correlation (R^2) was observed for all models based on their values were close to unity ($R^2 > 0.97$). This shows that the experimental values slump value, compaction factor, CS 28 d, split tensile strength, flexural strength and 28 d CP cannot be represented by the models only about 1.36%, 1.03%, 0.68%, 1.95%, 0.62%, and 0.07%, respectively.

3-dimensional (3D) response surface plot was used to illustrate the relationship between responses and independent variables. Figures 16–21 show the 3D response surface plots illustrating the relationship between responses (slump value, compaction factor, CS 28 d, split tensile strength, flexural strength and 28 d CP) and independent variables (W/C ratio and bentonite) for all mixes. The high-water absorption capacity of bentonite may have caused a rise in slump values with increasing w/c ratio, which decreases upon the addition of bentonite [12]. Bentocrete mixes exhibit Lower CS at early ages (7 d) curing, higher compressive strength at later curing period (28 d and 56 d). The reason behind this was the formation of secondary C–S–H gel since the bentonite obeys pozzolanic properties [42]. The split tensile strength and flexural strength of CM exhibits equal for 10BC for a few mixes, less strength was observed for 20BC and 30BC mixes. Bentocrete mixes display better durability upon addition of bentonite up to some extent (20%). This attributes the pore filling effect and happening of pozzolanic reaction caused by the addition of bentonite.

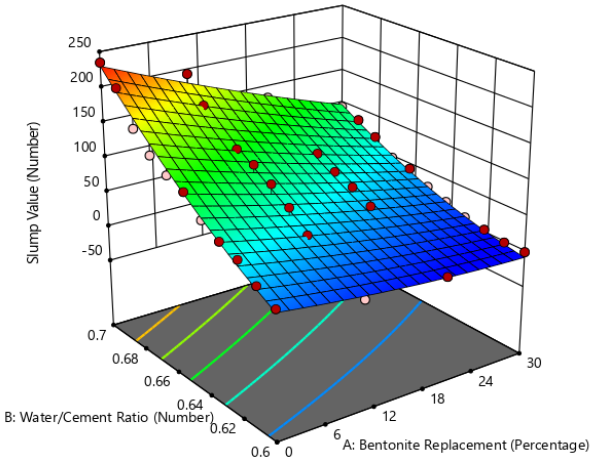

Figure 16. Response surface model for slump value.

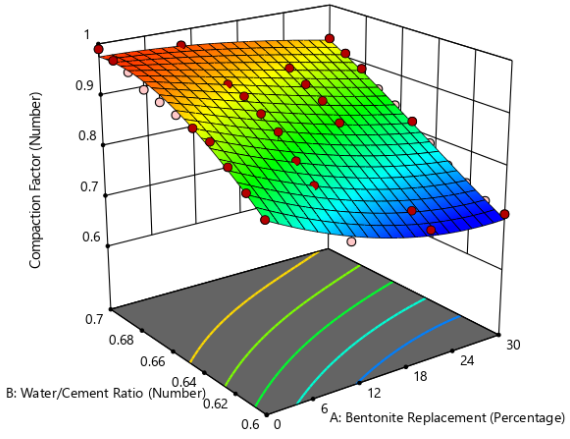

Figure 17. Response surface model for compaction factor.

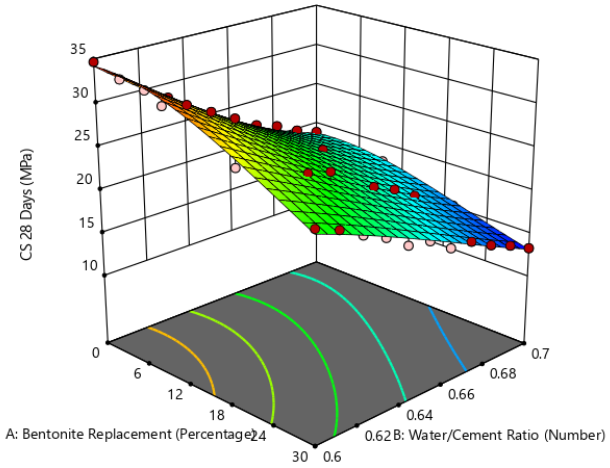

Figure 18. Response surface model for CS 28 d.

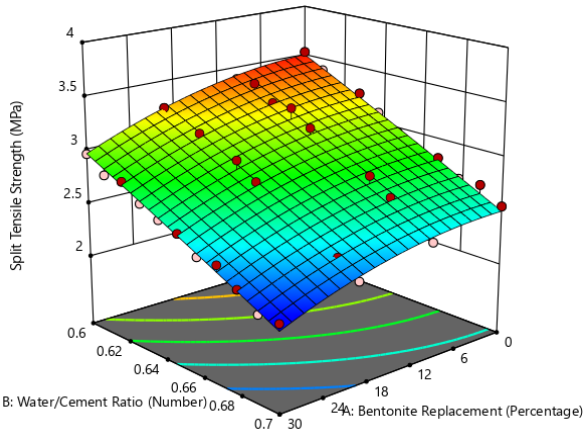

Figure 19. Response surface model for split tensile strength.

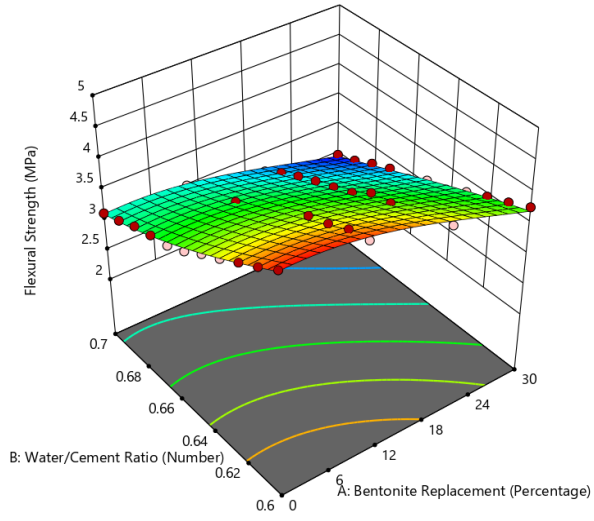

Figure 20. Response surface model for flexuleral strength.

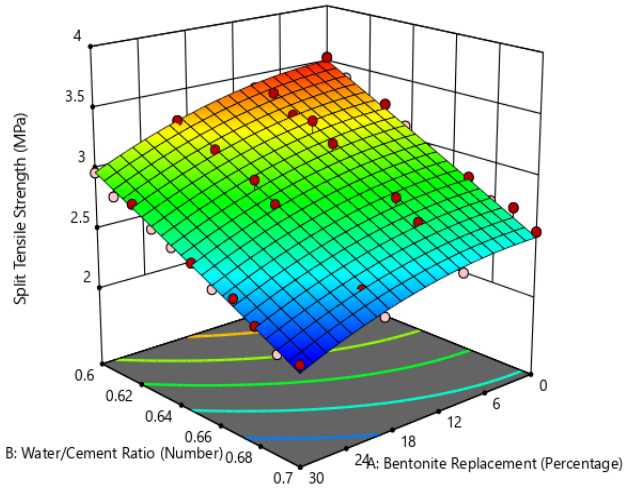

Figure 21. Response surface model for CP 28 d.

4.4. Optimization

Optimization was used with the aim of finding an optimized value among all mixes, performed by using Design Expert Software. The upper limit, lower limit and goal were set to perform the optimization, displayed in Table 12. The optimized solution was found with a desirability of 0.881, Table 13 shows the optimized Bentocrete mixes. The optimized mix was achieved at 3.92% of bentonite substitution and 0.62 W/C ratio. The optimum values of responses were 49.65 mm slump value, 0.85 compaction factor, 30.04 MPa CS 28 d, 3.28 MPa split tensile strength, 4.23 MPa flexural strength and 401.87 28 d CP.

Table 12. Criteria setting for optimization.

Variables/responses	Goal	Lower limit	Upper limit
Bentonite replacement	In range	0	30
W/C ratio	In range	0.60	0.70
Slump value	Target-50	0	235
Compaction factor	Target-0.85	0.71	173
CS 28 d	Maximize	13.33	34.65
Split tensile strength	Maximize	2.12	3.53
Flexural strength	Maximize	2.47	4.63
28 d CP	Minimize	367.5	691.75

Table 13. Optimized Bentocrete mixes.

Bentonite replacement	W-C ratio	Slump value	Compaction factor	CS 28 d	Split tensile strength	Flexural strength	28 d CP
3.92	0.62	49.65	0.85	30.04	3.28	4.23	401.87

5. Conclusions

The following conclusions were drawn based on the experiments and analyses performed: The standard consistency of cement paste is directly proportional to the bentonite substitution. 10 BC showed maximum compressive strength among all cement mortar mixes due to pozzolanic nature of bentonite. Workability is directly proportional to W/C ratio, because of the high-water absorption capacity of bentonite. The compression strength of Bentocrete shown lesser at 7 d equals at 28 d, and higher at 56 d than cement concrete. However, Bentocrete with more than 20 percentage of bentonite exhibits lesser compressive strength than concrete at all curing periods. In split tensile strength and flexural strength, the lower performance was observed for more than 10% of bentonite substitution. The durability against chloride ion was improved for Bentocrete than cement concrete up to 20% upon curing for enough time; this attribute the pore filling effect since bentonite's particle size is lesser than cement. Cost analysis was performed, 9.91% of the cost can be cut down for Bentocrete with 20 percentage bentonite. The RSM model has fitted the experimental data with the full agreement with R^2 values not less than 0.985 in all the cases. 3.92 % of bentonite substitution and 0.62 W/C ratio provided optimum solution for the intended goals with desirability of 0.881.

Acknowledgments

The authors are thankful to the authorities of the Koneru Lakshmaiah Education Foundation for funding this research as a part of the internal funding project scheme.

Conflict of interest

All authors declare no conflicts of interest in this paper.

References

1. Zeng Q, Li K, Fen-Chong T, et al. (2012) Determination of cement hydration and pozzolanic reaction extents for fly-ash cement pastes. *Constr Build Mater* 27: 560–569.
2. Heikal M, Eldidamony H, Helmy IM, et al. (2003) Pozzolanic activity of fly ash. Silic Ind 68: 111–117.
3. Mirza J, Riaz M, Naseer A, et al. (2009) Pakistani bentonite in mortars and concrete as low cost construction material. *Appl Clay Sci* 45: 220–226.
4. Memon SA, Arsalan R, Khan S, et al. (2012) Utilization of Pakistani bentonite as partial replacement of cement in concrete. *Constr Build Mater* 30: 237–242.
5. Ahmad S, Barbhuiya SA, Elahi A (2011) Effect of Pakistani bentonite on properties of mortar and concrete. *Clay Miner* 46: 85–92.
6. Masood B, Elahi A, Barbhuiya S, et al. (2020) Mechanical and durability performance of recycled aggregate concrete incorporating low calcium bentonite. *Constr Build Mater* 237: 117760.
7. Siddique R (2014) Utilization of industrial by-products in concrete. *Procedia Eng* 95: 335–347.
8. Nizar K, Kamarudin H, Idris MS, et al. (2007) Pysical, chemical & mineralogical properties of fly-ash. *J Nucl Rela Technol* 4: 47–51.
9. Cinku K, Karakas F, Boylu F (2014) Effect of calcinated magnesite on rheology of bentonite suspensions. Magnesia-bentonite interaction. *Physicochem Probl Mi* 50: 453–466.
10. Shabab ME, Shahzada K, Gencturk B, et al. (2016) Synergistic effect of fly ash and bentonite as partial replacement of cement in mass concrete. *KSCE J Civ Eng* 20: 1987–1995.
11. Latawiec R, Woyciechowski P, Kowalski K (2018) Sustainable concrete performance—CO_2-emission. *Environments* 5: 27.
12. Murray HH (2006) Bentonite applications, *Developments in Clay Science*, Elsevier, 2: 111–130.
13. Government of India Ministry of Mines Indian Bureau of Mines (2015) Bentonite, *Indian Minerals Yearbook 2013*, 52 Eds.
14. Reddy MAK, Rao VR (2019) Utilization of Bentonite in concrete: A review. *IJRTE* 7: 541–545.
15. Khushnood RA, Rizwan SA, Memon SA, et al. (2014) Experimental investigation on use of wheat straw ash and Bentonite in self-compacting cementitious system. *Adv Mater Sci Eng* 2014: 832508.
16. Afzal S, Shahzada K, Fahad M, et al. (2014) Assessment of early-age autogenous shrinkage strains in concrete using bentonite clay as internal curing technique. *Constr Build Mater* 66: 403–409.
17. Man X, Aminul Haque M, Chen B (2019) Engineering properties and microstructure analysis of magnesium phosphate cement mortar containing bentonite clay. *Constr Build Mater* 227: 116656.
18. Reddy GVK, Rao VR, Reddy MAK (2017) Experimental investigation of strength parameters of cement and concrete by partial replacement of cement with Indian calcium bentonite. Int J Civ Eng Technol 8: 512–518.
19. Wei J, Gencturk B (2019) Hydration of ternary Portland cement blends containing metakaolin and sodium bentonite. *Cem Concr Res* 123: 105772.

20. Şimşek B, Iç YT, Şimşek EH, et al. (2014) Development of a graphical user interface for determining the optimal mixture parameters of normal weight concretes: A response surface methodology based quadratic programming approach. *Chemometr Intell Lab* 136: 1–9.
21. Neville AM (2009) *Properties of Concrete*, 2 Eds., Person Education Limited.
22. Javed U, Khushnood RA, Memon SA, et al. (2020) Sustainable incorporation of lime-bentonite clay composite for production of ecofriendly bricks. J *Clean Prod* 263: 121469.
23. Divyana R (2015) An experimental study on concrete using bentonite and steel slag. *National Conference on Research Advances in Communication*, *Computation*, *Electrical Science and Structures*.
24. Chamundeeswari J (2012) Experimental study on partial replacement of cement by bentonite in paverblock. *Int J Eng Trends Technol* 3: 41–47.
25. Ahad MZ, Ashraf M, Kumar R, et al. (2018) Thermal, physico-chemical, and mechanical behaviour of mass concrete with hybrid blends of bentonite and fly ash. *Materials* 12: 60.
26. Adeboje AO, Kupolati WK, Sadiku ER, et al. (2020) Experimental investigation of modified bentonite clay-crumb rubber concrete. *Constr Build Mater* 233: 117187.
27. Chandrakanth M, Rao NPC, Rao KS (2016) Experimental studies on concrete with Bentonite as mineral admixture. *GRD J* 1: 7–10.
28. Karthikeyan M, Ramachandran PR, Nandhini A, et al. (2015) Application on partial substitute of cement by bentonite in concrete. *Int J ChemTech Res* 8: 384–388.
29. Sudheer KS, Kumar PPS, Reddy MAK, et al. (2017) A study on durability of concrete by partial replacement of cement with bentonite. *Int J ChemTech Res* 10: 898–904.
30. Karunarathne VK, Paul SC, Šavija B (2019) Development of nano-SiO_2 and Bentonite-based mortars for corrosion protection of reinforcing steel. *Materials* 12: 2622.
31. Xie Y, Li J, Lu Z, et al. (2018) Effects of bentonite slurry on air-void structure and properties of foamed concrete. *Constr Build Mater* 179: 207–219.
32. Klaus H, Oscar K (2018) *Design and Analysis of Experiments*, New York: John Wiley & Sons.
33. Mohammed BS, Liew MS, Alaloul WS, et al. (2018) Properties of nano-silica modified pervious concrete. *Case Stud Constr Mater* 8: 409–422.
34. Sun Y, Yu R, Shui Z, et al. (2019) Understanding the porous aggregates carrier effect on reducing autogenous shrinkage of Ultra-High Performance Concrete (UHPC) based on response surface method. *Constr Build Mater* 222: 130–141.
35. Ferdosian I, Camões A (2017) Eco-efficient ultra-high performance concrete development by means of response surface methodology. *Cem Concr Compos* 84: 146–156.
36. Ghafari E, Costa H, Júlio E (2014) RSM-based model to predict the performance of self-compacting UHPC reinforced with hybrid steel micro-fibers. *Constr Build Mater* 66: 375–383.
37. Mohammed BS, Adamu M, Liew MS (2018) Evaluating the effect of crumb rubber and nano silica on the properties of high volume fly ash roller compacted concrete pavement using non-destructive techniques. *Case Stud Constr Mater* 8: 380–391.
38. Mohammed BS, Achara BE, Liew MS, et al. (2019) Effects of elevated temperature on the tensile properties of NS-modified self-consolidating engineered cementitious composites and property optimization using response surface methodology (RSM). *Constr Build Mater* 206: 449–469.

39. Gao Y, Xu J, Luo X, et al. (2016) Experiment research on mix design and early mechanical performance of alkali-activated slag using response surface methodology (RSM). *Ceram Int* 42: 11666–11673.
40. Long X, Cai L, Li W (2019) RSM-based assessment of pavement concrete mechanical properties under joint action of corrosion, fatigue, and fiber content. *Constr Build Mater* 197: 406–420.
41. Montgomery DC (2017) *Design and Analysis of Experiments*, John Wiley & Sons.
42. Kadar JMA, Dhanalakshmi G (2016) Experimental investigation on concrete by partial replacement on cement by bentonite and coarse aggregate by steel slag. *IJIRSET* 5: 10302–10309.

AIMS Press